Curvature adaptive optics and low light imaging

Christ Ftaclas[1], Mark Chun[2], Jeffrey Kuhn[1,3], Joseph Ritter[3]
Institute for Astronomy, University of Hawaii

ABSTRACT

We review the basic approach of curvature adaptive optics (AO) and show how its many advantages arise. A curvature wave front sensor (WFS) measures exactly what a curvature deformable mirror (DM) generates. This leads to the computational and operational simplicity of a nearly diagonal control matrix. The DM automatically reconstructs the wave front based on WFS curvature measurements. Thus, there is no formal wave front reconstruction. This poses an interesting challenge to post-processing of AO images. Physical continuity of the DM and the reconstruction of phase from wave front curvature data assure that each actuated region of the DM corrects local phase, tip-tilt and focus. This gain in per-channel correction efficiency, combined with the need for only one pixel per channel detector reads in the WFS allows the use of photon counting detectors for wave front sensing. We note that the use of photon counting detectors implies penalty-free combination of correction channels either in the WFS or on the DM. This effectively decouples bright and faint source performance in that one no longer predicts the other. The application of curvature AO to the low light moving target detection problem, and explore the resulting challenges to components and control systems. Rapidly moving targets impose high-speed operation posing new requirements unique to curvature components. On the plus side, curvature wave front sensors, unlike their Shack-Hartmann counterparts, are tunable for optimum sensitivity to seeing and we are examining autonomous optimization of the WFS to respond to rapid changes in seeing.

Introduction

Adaptive correction of distorted or turbulent wave fronts is of growing importance to many civilian and military applications. In the military arena, Space Situational Awareness (SSA) is an important mission area where adaptive optics (AO) makes a fundamental contribution. SSA taxes the limits of imaging science. The combination of target proper motion, apparent size and integrated total magnitude define a daunting parameter space. Ground-based facilities bring operational and cost advantages to bear on the problem but they must all cope with the wave front decorrelations imposed on light traveling through the earth's atmosphere. Adaptive optics (AO), often with significant image post-processing, tries to recover the resolving power of large apertures to the degree that system noise sources permit. Functionally, however, we must use information (i.e. photons), generally from the target itself, to restore diffraction-limited performance. This need to consume photons for wave front sensing imposes its own limits on the observation. Almost universally, observations are limited not because the object is too faint to see but because it is too faint to correct.

Laser beacons projecting artificial stars on the sky can improve the photon flux available for wave front sensing but at the cost of a new level of complexity and compromised performance compared to natural guide star systems. Moreover, we still need target photons to fix image motion and focus and, operationally, illumination with laser light may not be appropriate for all targets. Curvature adaptive optics offers the potential of a significant gain in the ground-based contribution to SSA by extending adaptive correction to faint objects without the use of laser beacons. Curvature AO is intrinsically more efficient in terms of the number of channels needed for a given level of correction so that even when implemented with a laser beacon, there is significantly reduction in laser power requirements [1].

---

[1] IfA Manoa, 2680 Woodlawn Drive, Honolulu, HI 96822

[2] IfA Hilo, 640 North A'ohoku Place, Hilo, Hawaii 96720-2700

[3] IfA Maui, 34 Ohia Ku St. Pukalani, Hawaii 96768-8288

Curvature AO in the high Strehl domain is still a relatively young field. This is especially evident in the spectrum of available high performance curvature components. To our knowledge, we are the only group in the world actively researching and developing curvature components that would be the core of future systems. In the sections below, we will describe how curvature correction works, review its many advantages and show its potential contribution to the SSA problem.

Curvature Adaptive Correction

Most AO systems in the world use a slope measuring (Shack-Hartmann, SH) wave front sensor (WFS) combined with a deformable mirror (DM) that pushes and pulls locally on a thin face-sheet to make phase corrections. Because the WFS measures slopes but the DM corrects phase there is a level of computational complexity and algorithmic ambiguity associated with phase reconstruction. Curvature AO is an alternative to this approach that begins with the fundamental simplicity that the WFS measures exactly the signal the DM produces: wave front curvature. Francois Roddier [2] invented the curvature measuring sensor concept[i] and led his group at the Institute for Astronomy in developing a system based on it [3]. Curvature systems are so radically different in their fundamental approach and implementation that much of the traditional AO knowledge and experience is of little help in understanding, designing and operating them. A small but growing curvature community is centered primarily Hawaii and at the European Southern Observatory.

Initially, the AO community viewed curvature AO as a low order modal correction scheme to remove a few Zernike polynomials and hand-waving arguments purported to show that performance could never go much beyond that level. That changed rather dramatically in 2000 when the UH group demonstrated correction to the diffraction limit on an eight-meter telescope with only a 36-channel system [4] (Hokupa'a-36[4]) and there was more interest in curvature wave front correction. ESO for example has built and deployed built five, 60-channel systems. The two 85-channel systems built at IfA were the largest in the world until Subaru began commissioning this year on its 188-channel system. Our own research [5] has shown that models for RC systems in excess of 500 channels do not exhibit any fall off in correction efficiency compared to low order systems.

The Subaru 188 channel DM would stand as the benchmark in the development f curvature deformable mirrors except that its resonant frequency (~200Hz) is so low it cannot operate in the SSA domain. The highest performance curvature deformable mirror demonstrated to date is the one built at IfA that is installed in the Gemini Near Infrared Coronagraph (NICI) with a resonant frequency five times that of the Subaru DM.

Functionally, a curvature AO system looks like any other closed loop control system but the WFS and DM implementations are unique to curvature AO. In principle, one can use either the curvature WFS or DM as separate components but pairing them yields advantages not found in either component. We will refer to traditional AO systems as Shack-Hartmann or **SH** type and to curvature systems as Roddier–Curvature or **RC** type. An RC WFS (pictured in Fig. 1) works by comparing images taken on either side of focal or pupil planes. The basic idea is that wave front curvature causes portions of the pupil to focus early or late relative to the mean focus resulting in intensity differences between intra- and extra-focal images. We form the signal:

$$S = \frac{I - E}{I + E},$$

where *I* and *E* refer to the intra- and extra-focal images respectively. The *I* and *E* images fall on a lenslet array (Fig. 2) whose elements define the WFS channels. We have to make two measurements per correction cycle but only one sensing element is required per measurement/per channel as opposed to SH systems where we need at least four sensing elements to sense spot displacement. In our systems, the lenslet array achromatically images light onto a set of optical fibers that each feed a photon counting avalanche photo diode (APD, Fig. 3). At the edge of the beam, the signal *S,* corresponds to the radial components of the wave front slope since radial edge slope moves the beam edge in the opposite sense in each extra-focal image.

[4] Hokupa`a means fixed or unmoving star in Hawaiian and is often applied to Polaris.

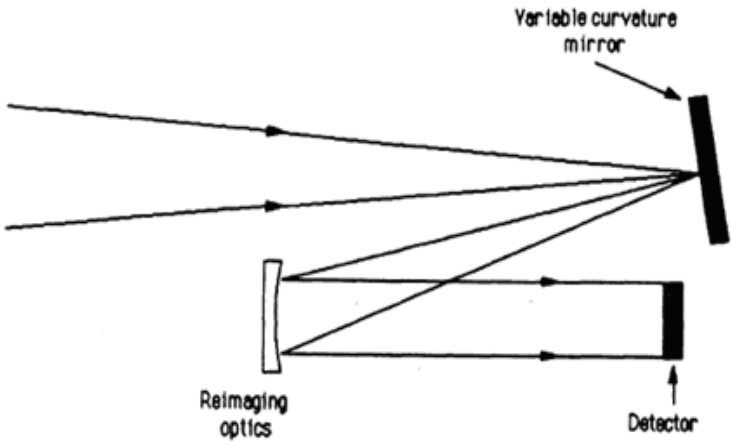

Fig. 1 Optical System for Curvature Sensing. The variable curvature mirror is an acoustically driven, vibrating membrane at the telescope focus. The detector plane is a pupil image when the membrane is flat. When the membrane is driven, it alternately images intra- and extra-focal images onto the detector (taken from *Error! Bookmark not defined.****). A major advantage of this design is that as the membrane mirror stroke modifies the extra-focal distance, the size of the extra-focal images remains constant.***

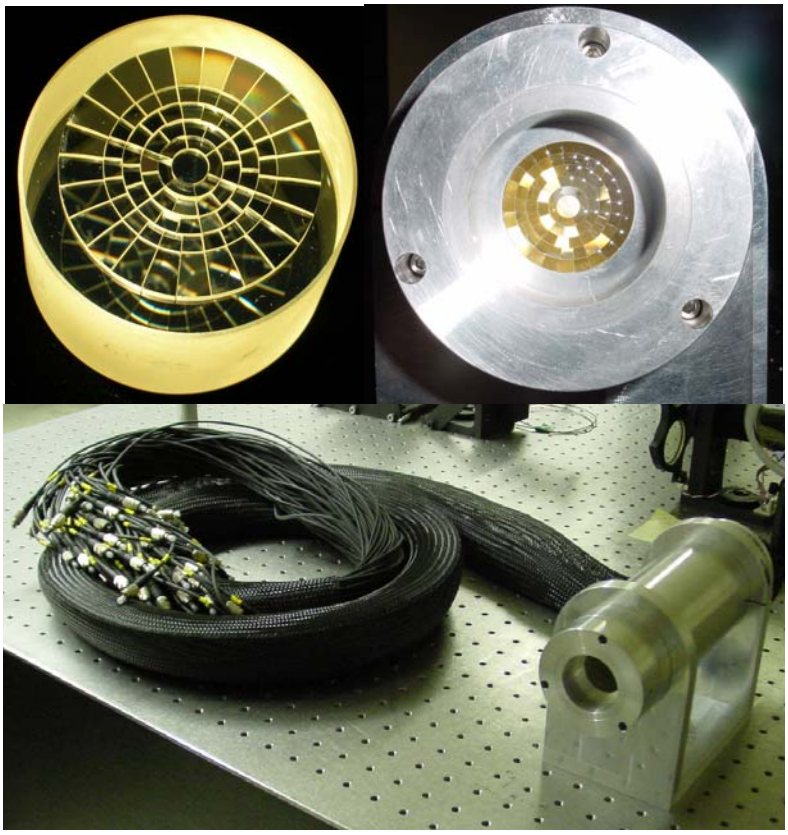

Fig. 2. Top left: an 85-element lenslet array –The shape of each segment is a copy of the corresponding actuator on the DM. The combination of lenslet and mounting cylinder glasses achromatizes the lenslet focus over the entire visible spectrum. Top right: a face-on view of the mounted lenslet array. Bottom: A complete lenslet assembly showing the bundle of 85 optical fibers associated with the lenslet segments.

Unlike the SH WFS, there is an additional degree of freedom in RC wave front sensing: we can alter how far out of focus the analyzed WFS images are by altering the amplitude of the membrane mirror. This alters the size of the response of the WFS to a given curvature signal and allows tuning the WFS as atmospheric conditions vary. Increasing the residual WFS signal also decreases the shot noise in the signal so the system signal to noise improves. In a SH system this is equivalent to changing the focal length or equivalently, the pitch of the lenslet array and is very difficult to accomplish. In RC systems, it is simple to do and, in principle, can be automated.

The information contained in the distribution of *S* over the beam is sufficient for the DM to reconstruct the wave front. Moreover, the measured signal *S* corresponds exactly to what the curvature deformable mirror generates so that we have a nearly diagonal control matrix. When we actuate the DM with the control voltages derived from the WFS readings, it takes on the curvature and edge slope distribution measured by the WFS. This information, together with the mechanically imposed surface and slope continuity of the DM is sufficient for the DM to reconstruct the input wave front error. The control system only commands the local focus or edge slope at the DM but the DM reconstructs the entire wave front. It follows that in addition to local focus, we also correct the local slope as well as the phase itself. Consequently, **each RC actuator region is the equivalent of several SH push-pull actuators.**

In curvature systems, the WFS-DM combination acts like an analog computer for wave front reconstruction. With each channel correcting local focus, slope and phase we only need about one-third the channels needed in an SH system to achieve the same level of performance on a given guide star [6]. Researchers noted early on in developing RC systems that combining high DM correction efficiency (fewer channels of correction needed) with a curvature WFS (only a single sensing element per channel) meant that at least an order of magnitude fewer WFS detector elements were necessary in RC systems compared to SH systems. This made it practical to use photon-counting detectors on each channel. This not only enables low light operation but also allows noiseless channel combination, further improving faint source response.

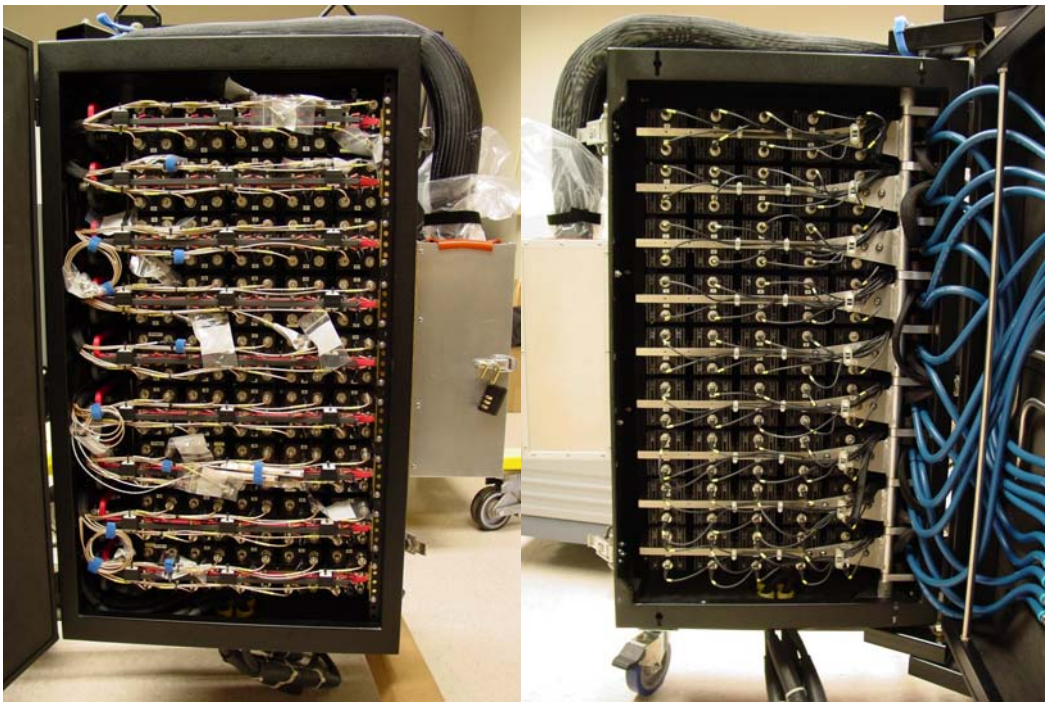

Fig. 3. Two views of the Avalanche Photo-Diode Cabinet. On the left, the rear door is open and one can see the power and signal out connections. On the right, the front door is open showing the fiber connections from the lenslet array and the coolant circulation system. The APD's are mounted on nine swing-out shelves with 10 APDs per shelf. (Spares permit observations to go on in case of APD failure.) Each shelf has internal channels for circulating coolant. Inside the cabinet, we monitor the dew point to prevent condensation.

3. Curvature Deformable Mirrors

We know the piezoelectric effect as a way to sense and control position. Applying an electric field along the polarization direction of a piece of PZT produces a strain along that direction and inversely, a strain produces a voltage across the PZT. Less well known, however, is that this process roughly conserves volume so that if the PZT thickens along the poled axis, it will also contract in the plane orthogonal to the poled axis. For an electric field along the poled axis the diagonal values of the strain are:

$$\varepsilon_3 = d_{33}E_3, \quad \varepsilon_1 = d_{13}E_3, \quad \varepsilon_2 = d_{23}E_3, \quad d_{13} = d_{23} \approx -\frac{1}{2}d_{33}$$

where d_{ij} is the matrix of material piezoelectric constants and E_3 is the *z*-component of the electric field. The diagonal elements of the strain sum approximately to zero, conserving volume. Generating a strain along the poled direction is the *direct* piezoelectric effect and the associated strain in the plane orthogonal to the poled direction is the *transverse* piezoelectric effect.

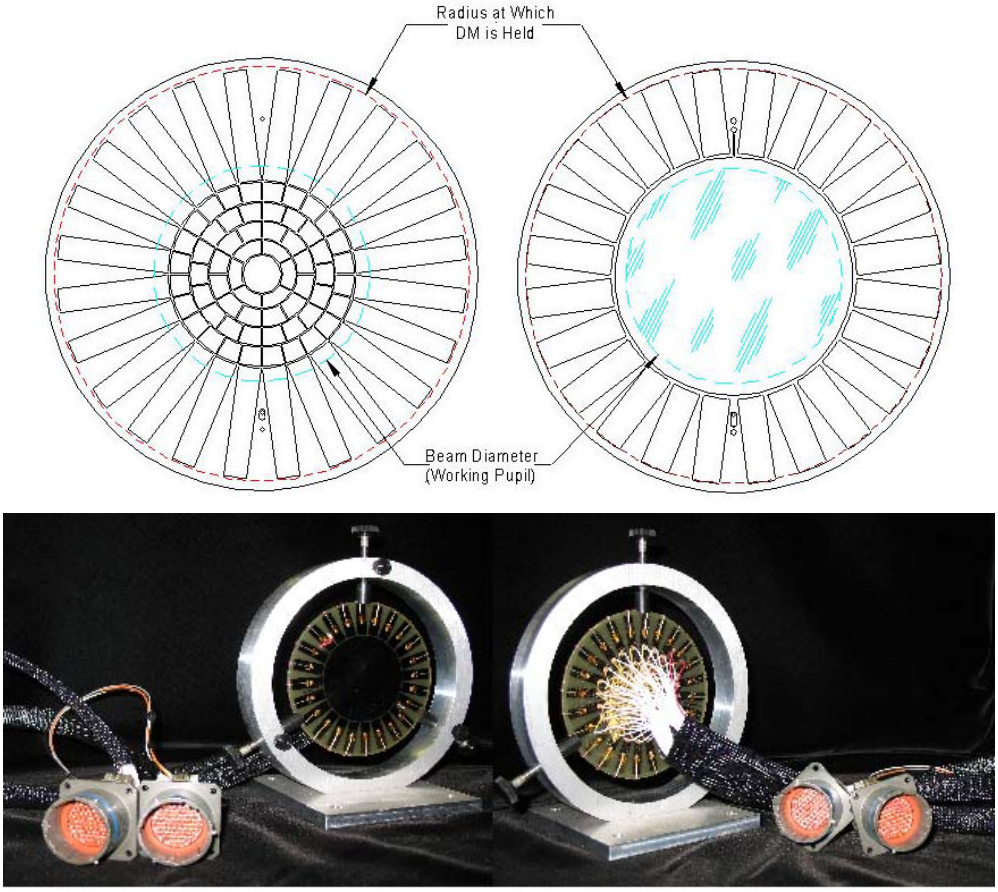

Fig. 4 (Top) Back (left) and Front (right) actuator patterns of our 85-element deformable mirror. The smaller curvature actuators operate in a unimorph mode. The long edge actuators are on both sides operate as a cooperative bimorph essentially doubling the curvature that can be achieved. (Bottom) Front (left) and back (right) views of a completed DM. The mount shown is a 3-point lab test cell. In practice, we hold the DM between two o-rings that constrain it over its entire circumference.

The curvature DM (Fig. 4) is a thin bonded sandwich of piezoelectric material poled through the thickness with a central ground layer and lithographically applied electrodes on both sides. The front electrodes include a large central focus electrode that is the *mirror* part of the DM. It is slightly larger than the reimaged system pupil. The back electrode pattern is a copy of the lenslet pattern (Fig. 2). We hold the DM only at its edge, captured

between two O-rings that constrain its *z*-motion. The small electrodes on the back surface of the DM act entirely within the pupil are curvature actuators. The long electrodes that are mostly outside the pupil and run to the constrained edge of the DM are edge benders.

When we apply voltage to a curvature electrode, it creates a local electric field through the thickness of the disk. The strain $\frac{\delta\ell}{\ell}$ is largest along the poled direction but ℓ, the wafer thickness, is smallest in this direction compared to the electrode dimensions. Therefore, the dominant dimensional change is due to the transverse piezoelectric effect and the PZT between the electrode and the ground layer wants to expand or contract uniformly in the *x-y* plane. The front half of the bonded sandwich resists this motion causing the activated electrode to curve against the passive front half of the DM. This mode of action is *unimorph* activation. Each edge-bending electrode appears on both the front and back of the DM. The two pieces of the electrode are electrically continuous so applying voltage to an edge bender results in oppositely directed electric fields in each DM half. We assemble the DM with the poling vectors of the two halves parallel so the strains in the front and back halves of the DM are opposite in sign and cooperate in producing a curvature about twice that produced by the curvature electrodes. This is *bimorph* activation of the DM. The long shape of the edge benders results in an action that primarily bends the pupil edge against the fixed boundary condition at the DM edge.

Mathematically speaking, the fixed edge of the DM provides Neumann boundary conditions to the entire DM surface while the edge benders apply Dirichlet boundary conditions to the working pupil. These boundary conditions combined with the measured curvature distribution over the pupil enable the solution for the wavefront on the DM surface. The action of any given DM actuator changes the surface height and slope distributions everywhere in the pupil, which would completely confound a SH system. The RC WFS, however, only sees the DM in curvature so that the DM action looks local and the control matrix is system or interaction matrix is nearly diagonal.

4. What does Curvature AO bring to SSA and the AEOS Facility

The performance of the AEOS system depends, of course on, atmospheric conditions as well as many other factors. The general sense, however, is that AEOS obtains very high Strehl ratios on bright stars and that Strehl ratios degrade relatively rapidly for stars fainter than 6th magnitude [7] We will refer to this as the effective performance limit although we recognize that Strehl depends on many factors. In this section, we examine the potential gains from a curvature AO system applied to the SSA problem at AEOS.

Based on the discussion above we can summarize the pertinent advantages of RC AO systems as:

- Only one sensing element required per WFS channel
- Interaction and control matrices are nearly diagonal - the WFS measures exactly what the DM creates
- The sensitivity of the WFS is tunable in real time as atmospheric conditions change.
- No formal wave front reconstruction is required.
- Each channel corrects local phase, tip-tilt and focus (curvature) although we make only one WFS measurement per channel.
- Each channel can be photon counting allowing noiseless channel combination.

With fewer channels required and each channel photon-counting it is clear why RC systems are optimal for low light operation. Add to this a sparse, nearly diagonal control matrix, no need for a formal reconstructor and we can see that RC systems are also be optimized for speed. The computational overhead is so low on typical RC systems that they run with Pentium class computers. High speed and low light sensitivity are certainly critical attribute in assessing performance in the SSA parameter space.

To go further we consider a performance data point for our 85-channel RC system on the AEOS telescope (Fig. 5). The models are for an unresolved point source imaged at $\lambda = 0.85\mu\text{m}$ and have no correction for system throughput (~1.5-2mag). They show that an enormous gain in low light performance relative to the current AEOS system is potentially possible with RC systems. The models illustrate the shot noise and fitting error performance limits and we are working to develop estimates that are more realistic and to extend these estimates to the high-speed domain of rapidly moving extended objects.

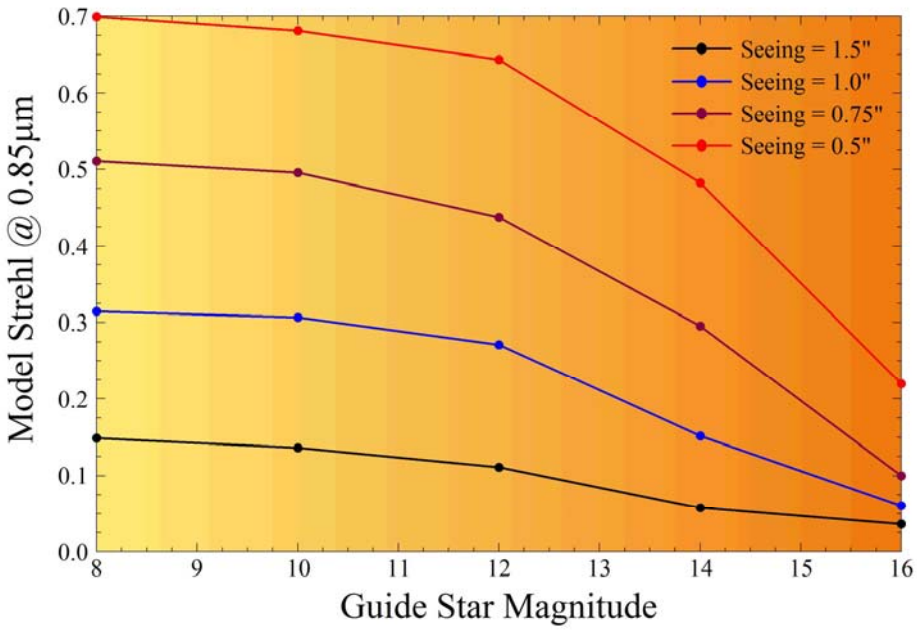

Fig. 5 Expected point source model Strehl from an 85-element curvature AO system on AEOS. In each case AO settings have been optimized for seeing and guide star magnitude. The Strehl is relatively flat for stars brighter than eighth magnitude indicating that measurement noise in the WFS is no longer the dominant residual error.

It is encouraging that the AEOS faint object limit of $m_V = 6$ is off the bright edge of this plot but we must also look at bright star performance. The curves plotted in Fig. 5 would continue nearly horizontally for brighter guide stars since getting more photons generally would not increase performance unless the system bandwith was also increased. Thus, our 85-channel system would seriously underperform relative to the current system for bright objects. This suggests perhaps a hybrid system but there is a more efficient way to go. As we have noted, photon-counting detectors in the WFS permit noiseless channel combination. This can be either explicit in the control computer or passive by applying noisy estimates and letting the DM average over them. The key issue is that if we were to take any curve plotted in Fig. 5 and then generate the curve for the same conditions but vary the number of actuators all curves would be asymptotic to one another at the faint limit because there is no read noise in the WFS.

We can envision a curvature adaptive system with enough actuators to reproduce the AEOS bright star performance and we know that the faint star model performance would be no worse than that in Fig. 5 for the same seeing and wind speed. In looking at a family of high order curvature systems [5], we found that a single phase transfer function scaled for seeing and the system Nyquist frequency described all the systems[Error! Bookmark not defined.]. Whether we use this transfer function or the general rule of a 3:1 equivalence in actuator count between RC and SH systems we get an estimate of 250-300 actuators for the RC system that would reproduce AEOS bright star behavior. This system, however, would also have a faint star performance given by Fig. 5 and it would happen almost automatically.

5. Conclusion

We envision a curvature adaptive system with 250-300 channels implementing a photon-counting WFS. A single system that will reproduce the bright star performance of the current AEOS system but extend closed loop performance to guide stars more than a hundred times fainter than the current system. The majority of technologies used in building RC systems are scalable to larger systems in principle, but looking at the volume, weight and electrical infrastructure required for the APDs, for example (Fig. 3), simply scaling to several hundred channels is not feasible for an instrument that would hang on a telescope. The Subaru 188-channel system is about the practical limit for using APDs. The AEOS Coudé experiment room architecture, however, virtually eliminates weight/volume concerns. Progress in photon counting APD arrays and other detectors types could alter this consideration in the future, but we know that, for now, the detectors are not a concern and are available.

Fig. 6. Hokupa'a 85 (in the lab, left), one of the e85 element systems built at the IfA. It is an 85-channel adaptive relay designed to mount directly on the telescope (right). The APD enclosure is on the left side of the mounted instrument and the large blue box on the right side of the instrument holds the electronics for actuating the DM and for counting and processing pulses from the APDs.

Our group at the IfA has already built two systems for the Gemini South eight-meter telescope: an 85 channel adaptive relay (Hokupa'a-85, Fig. 6) and another 85-channel system for the Gemini South Near-Infrared Coronagraphic Imager (NICI) and feel we can identify the technical drivers for a system like this. At this time, the critical issue for this high-performance system is the curvature deformable mirror. Our current deformable mirror has a minimum radius of curvature of 10 meters. For a 300-actuator system and seeing of 1.5 arc-seconds, however, we need a minimum radius of curvature of 6.5 meters. So we need a DM with an actuator density 3-4 times that of our current mirrors and a radius of curvature about half of our current mirrors. We think we know how to do this and have already demonstrated many of the key technologies.

References

[1] **Curvature-Based Laser Guide Star Adaptive Optics System For Gemini South**, M. Chun et al, *Proc. SPIE* Vol. 4007, p. 142-148, Adaptive Optical Systems Technology, Peter L. Wizinowich; Ed.

[2]F. Roddier, **Curvature Sensing And Compensation: A New Concept In Adaptive Optics**, *Applied Optics* **27**,1223(1988).

[3] F. Roddier, M. Northcott and J. E. Graves, **A Simple Low-Order Adaptive Optics System for Near Infrared Applications** *PASP* **103,** 131 (1991) .

[4] E. Graves et al, **First Light For Hokupa'a 36 On Gemini North**, *Proc SPIE* **4007**, 26 (2000)

[5] **Wavefront Correction with High Order Curvature Adaptive Optics System**s Yang, Q, C. Ftaclas and M. Chun, 2006, *Journal of the Optical Society of America* **23,** 1375-1381.

[6] **Comparison of Curvature-based and Shack-Hartmann-based Adaptive Optics for the Gemini Telescope.** F.R.Rigaut, B.L. Ellerbroek and M.J. Northcott, *Applied Optics* **36,** 2856 (1997)

[7] **Characterization of the AEOS Adaptive Optics System.** L.C.Roberts, C.R. Neyman, *PASP* **114,** 1260(2002).